IFERP connecting engineers... developing research

ISSN (Online) 2456-1290

International Journal of Engineering Research in Mechanical and Civil Engineering (IJERMCE)

Vol 2, Issue 4, April 2017

Study on Thermo-Hydrodynamic Performance of a Finite Porous Journal Bearing

[1] Mohammedrafi H. Kerur, [2] T. Nagaraju, [3] M. Ravi Prakash
[1], [2], [3] Department of Mechanical Engineering, P E S College of Engineering, Mandya-571401, India

Abstract: **-- — The present theoretical study predicts the static and dynamic performance characteristics of porous journal bearing considering rise in fluid film temperature. The modified Reynolds equation governing the pressure field within fluid-film is derived by simplifying the Navier-Stokes equation. The modified energy equations governing the temperature fields are also derived for both fluid film and porous medium. The modified Reynolds and energy equations are simultaneously solved using finite element method with appropriate iterative schemes. The influence of permeability of porous matrix on static and dynamic performance characteristics of porous journal bearing is computed using thermo-hydrodynamic (THD) analysis and compared with the isothermal performance characteristics of the same bearing. The performance parameters of finite porous journal bearings under THD analysis were found to be significantly influenced by the permeability of porous matrix. The influence of permeability of porous matrix has observed to couple with operating eccentricity, speed of journal and temperature effects.**

Index Terms **— Finite element method, performance characteristics, Porous journal bearing, Thermal effects.**

I.INTRODUCTION

Tribological systems needs continuous lubrication, temperature control and reduced friction for their smooth operation. It is commonly achieved by externally pressurised source that carries lubricant to the system and withdraws the used and heated lubricant away from the system. The circuit of a pressurized source usually consists of pumps, pipes and tubes and hence requires more space. Applications of externally pressurized sources, which are impractical due to the lack of space or inaccessible to lubrication, could be replaced by self-lubricating bearings called porous journal bearings. Porous journal bearing consist a metallic porous bush in which the lubricating oil is stored and feeds to the journal surface. Thus it avoids external oil supply for lubricating the contact surfaces of rotating shaft and the stationary bush.

Over the past decades, a considerable amount of theoretical studies on the performance characteristics of porous journal bearings have been carried out by several researchers. Most of these studies have been carried out using either Darcy's law or Brinkman extended Darcy equation. Lin and Hwang [1] used the Brinkman-extended Darcy model to analyze the hydrodynamic performance of short porous journal bearings. Reason and Siew [2] presented a numerical solution for the analysis of hydrodynamic performance of a finite porous journal bearing. Their solution takes into account the curvature of bearing wall, interfacial slip of the fluid across the pore mouths and employs the Reynolds boundary conditions at the oil film extremities. Guha [3], Naduvinamani and Siddangouda [4] and Naduvinamani and Patil [5] studied the effect of couple stress lubricant on performance of porous journal bearings. Shaheed [6] considered the combined influence of couple stress fluid and journal misalignment effects on static characteristics of porous journal bearing. Mak and Conway [7] and Elsharkawy and Guedouar [8], [9] carried out elastohydrodynamic lubrication analysis of porous journal bearings. Boubendir, Larbi and Bennacer [10] considered the thermal effects in the analysis of finite porous journal bearing with sealed ends. They derived the Reynolds equation by applying Darcy's law to include the rise in fluid film temperature. Their results indicate the considerable influence of temperature on the journal bearings performance. A progressive reduction in the pressure distribution, load capacity and attitude angle was found for increasing permeability. Except Boubendir, Larbi and Bennacer [10], none of the above studies considered the thermal effects in the analysis of porous journal bearing. Hence, more studies which consider the thermal effects in the analysis of porous journal bearings are still essential.

Therefore, the present study is aimed to carry out a theoretical study on THD performance of a finite porous journal bearing. The modified Reynolds and energy equations are developed to include the viscosity variation of fluid film due to its temperature rise.

II. MATHEMATICAL FORMULATIONS

Modified Reynolds Equation

For the fluid-film region of porous journal bearing system, the modified form of Reynolds equation is derived using Darcy's equation. It is expressed in non-dimensional form as

$$\frac{\partial}{\partial\alpha}\left[\left(\bar{h}^3\bar{F}_2+\frac{\bar{kh}}{\bar{\mu}}\frac{\bar{F}_1}{\bar{F}_0}\right)\frac{\partial\bar{p}}{\partial\alpha}\right]+\frac{\partial}{\partial\beta}\left[\left(\bar{h}^3\bar{F}_2+\frac{\bar{kh}}{\bar{\mu}}\frac{\bar{F}_1}{\bar{F}_0}\right)\frac{\partial\bar{p}}{\partial\beta}\right]$$

ISSN (Online) 2456-1290
International Journal of Engineering Research in Mechanical and Civil Engineering (IJERMCE)
Vol 2, Issue 4, April 2017

$$= \Omega_j \frac{\partial}{\partial \alpha}\left[\left(1-\frac{\overline{F}_1}{\overline{F}_0}\right)\overline{h}\right] + \Omega_j \frac{\partial \overline{h}}{\partial \overline{t}}$$
--- (1)

where $\overline{h}$ is the fluid film thickness and it is expressed as

$$\overline{h} = 1 - \overline{X}_j \cos\alpha - \overline{Z}_j \sin\alpha$$
--- (2)

Boundary Conditions

The following boundary conditions are used to solve Reynolds equation (1):

1. Nodes situated on the external boundary of the bearing have zero pressure, $\overline{P}\big|_{\beta=\pm 1.0} = 0.0$
2. At the supply hole, $\overline{p} = \overline{p}_s = 1$
3. At the trailing edge of the positive region, Reynolds boundary conditions are employed, $\overline{p} = \frac{\partial \overline{p}}{\partial \alpha} = 0$
4. At fluid film and porous bush interface, $\overline{p} = \overline{p}^*$

Energy Equation for Fluid-Film Media

The 3D energy equation is expressed in non-dimensional form as

$$\overline{h}^2\left[\overline{u}\frac{\partial \overline{T}_f}{\partial \alpha} + \overline{v}\frac{\partial \overline{T}_f}{\partial \beta} + \frac{\tilde{w}}{\overline{h}}\frac{\partial \overline{T}_f}{\partial \overline{z}}\right] = \overline{P}_f\left[\frac{\partial^2 \overline{T}_f}{\partial \overline{z}^2}\right] + \overline{D}_f \overline{\mu}\left[\left(\frac{\partial \overline{u}}{\partial \overline{z}}\right)^2 + \left(\frac{\partial \overline{v}}{\partial \overline{z}}\right)^2\right]$$
--- (3)

Energy Equation for Porous Media

For the porous media, the non-dimensional form of energy equation in cylindrical coordinate is expressed as

$$\overline{P}_p\left[\overline{u}^*\frac{1}{\overline{r}}\frac{\partial \overline{T}_p}{\partial \alpha} + \overline{v}^*\frac{\partial \overline{T}_p}{\partial \beta}\right] = \overline{K}_{ep}\left[\frac{\partial^2 \overline{T}_p^*}{\partial \overline{r}^2} + \frac{1}{\overline{r}}\frac{\partial \overline{T}_p^*}{\partial \overline{r}} + \frac{1}{\overline{r}^2}\frac{\partial^2 \overline{T}_p^*}{\partial \alpha^2} + \frac{\partial^2 \overline{T}_p^*}{\partial \beta^2}\right]$$
--- (4)

Temperature-Viscosity Relation

The fluid viscosity is assumed to be dependent on temperature and is defined by the exponential law. It is expressed in non-dimensional form as

$$\overline{\mu} = Exp\left[\overline{\beta}_v\left(\frac{\overline{T}_f + 273.12/T_r}{1+273.12/T_r} - 1\right)\right]$$
--- (5)

where $\overline{\beta}_v$ is the non-dimensional temperature-viscosity coefficient and is given by

$$\overline{\beta}_v = \beta_v\left(T_r\left(1+273.12/T_r\right)\right)$$

Load Carrying Capacity

The fluid film reaction components along x and z directions are given by

$$\overline{F}_x = -\int_{-\lambda}^{+\lambda}\int_0^{2\pi} \overline{p}_f \cos\alpha \, d\alpha d\beta \quad \overline{F}_z = -\int_{-\lambda}^{+\lambda}\int_0^{2\pi} \overline{p}_f \sin\alpha \, d\alpha d\beta$$
--- (6)

The resultant fluid film reaction is given by

$$\overline{F} = \left[\overline{F}_x^2 + \overline{F}_z^2\right]^{1/2}$$

For the bearing subjected to vertical load, the load carrying capacity at steady state condition is given by

$$\overline{F}_o = \overline{F}_z \text{ Since } \overline{F}_x = 0$$
--- (7)

Fluid-Film stiffness and Damping Coefficients

The linearized fluid film stiffness coefficient are defined as

$$\overline{S}_{ij} = -\frac{\partial \overline{F}_i}{\partial \overline{q}_j}; (i = x, z)$$
--- (8)

Where, subscript i represents the direction of fluid-film reaction and $\overline{q}j$ represents the displacement of journal centre ($\overline{q}_j = \overline{X}_j, \overline{Z}_j$).

Similarly, the linearized fluid-film damping coefficients defines as

$$\overline{C}_{ij} = -\frac{\partial \overline{F}_i}{\partial \dot{\overline{q}}_j}; (i = x, z)$$
--- (9)

Where, $\bar{q}_j = \bar{X}_j, \bar{Z}_j$ represents the velocity of journal centre.

Stability Threshold Speed Parameter

The linearized equations of motion of journal can be written as

$$\begin{bmatrix} \bar{M}_j & 0 \\ 0 & \bar{M}_j \end{bmatrix} \begin{Bmatrix} \ddot{\bar{X}}_j \\ \ddot{\bar{Z}}_j \end{Bmatrix} + \begin{bmatrix} \bar{C}_{xx} & \bar{C}_{xz} \\ \bar{C}_{zx} & \bar{C}_{zz} \end{bmatrix} \begin{Bmatrix} \dot{\bar{X}}_j \\ \dot{\bar{Z}}_j \end{Bmatrix} + \begin{bmatrix} \bar{S}_{xx} & \bar{S}_{xz} \\ \bar{S}_{zx} & \bar{S}_{zz} \end{bmatrix} \begin{Bmatrix} \bar{X}_j \\ \bar{Z}_j \end{Bmatrix} = \begin{Bmatrix} 0 \\ 0 \end{Bmatrix} \quad \text{--- (10)}$$

The characteristic equation is written for the above equation of motion and the critical or marginal value of journal mass ($\bar{M}_c$) for stability is obtained by satisfying the necessary and sufficient conditions Routh's stability criteria. Then stability threshold speed parameter is obtained by

$$\bar{\omega}_{th} = \left[\frac{\bar{M}_c}{\bar{F}_o} \right]^{1/2} \quad \text{--- (11)}$$

The journal is asymptotically stable when the journal mass is less than the critical mass (i.e. when $\bar{M}_j < \bar{M}_c$). Likewise, the journal is asymptotically stable when the operating speed of journal is less than the stability threshold speed of journal (i.e. when $\Omega_j < \bar{\omega}_{th}$).

III. RESULTS AND DISCUSSION

The modified Reynolds Eq. (1) and energy Eqs. (3) and (4) at fluid-film and porous matrix domains are simultaneously solved using finite element method and appropriate iterative schemes to get the converged fluid-film pressure and temperature fields. Once the converged pressure field is obtained, the static and dynamic performance characteristics of bearing are computed using the Eqs. (6) to (11).

The THD performance (both static and dynamic) characteristics of porous journal bearing are computed for the following non-dimensional operating and geometric parameters:

Aspect ratio, $\lambda = 1$

Eccentricity ratio, $\varepsilon = 0.3, 0.6, 0.8$

Speed parameter, $\Omega_j = 17.404$

Permeability parameter, $\bar{k} = 1 \times 10^{-8}$ to 1.0

Peclet number for porous bush, $\bar{P}_p = 1464.5$

Peclet number for fluid, $\bar{P}_f^* = 1.675$.

The static performance characteristic such as load carrying capacity ($\bar{F}_o$) and dynamic performance characteristics such as fluid-film direct stiffness coefficient ($\bar{S}_{xx}$) and damping coefficients ($\bar{C}xx$ and $\bar{C}_{zz}$) of finite porous journal bearing taking into account the effect of rise in fluid-film temperature are computed as a function of permeability parameter ($\bar{k}$), eccentricity ratio (ε) and speed parameter (Ω_j). These results are computed for both isothermal hydrodynamic (IHD) and thermohydrodynamic (THD) cases and compared.

Figure 1 shows the influence of permeability of porous matrix on load carrying capacity of porous journal bearing at different eccentricity ratios. The load carrying capacity of bearing reduces when temperature effect is considered (i.e. in THD analysis) due to decrease in fluid viscosity for rise in temperature. The load carrying capacity in both THD and IHD cases is observed to be constant up to certain permeability parameter and then it starts to reduce as permeability parameter increases. The range of permeability parameter up to which the load carrying capacity remains constant is shown to increase when temperature effect is considered. That is porous bearing with higher permeability is also shows almost same load carrying capacity as that of solid bearing. It may be noted that as the permeability parameter becomes smaller, the bearing acts as solid bearing.

Figure 2 shows the influence of permeability of porous matrix on load carrying capacity of porous journal bearing at different speed parameter for THD and IHD cases. As the viscous shear of lubricant increases with speed of journal, fluid-film temperature increases as the speed increases. Consequently fluid viscosity decreases and hence the load carrying capacity of bearing reduces as the speed of journal increases in THD case while it shows opposite trend in IHD case. The range of permeability parameter up to which its effect on load carrying of bearing is insignificant is observed to be increases as the speed increases in THD case while it remains almost same for all speed parameters considered in IHD case. Thus, the influence of permeability parameter is

ISSN (Online) 2456-1290
International Journal of Engineering Research in Mechanical and Civil Engineering (IJERMCE)
Vol 2, Issue 4, April 2017

observed to be coupled with the speed parameter when temperature effect is considered.

Figures 3 and 4 show the influence of permeability of porous matrix on direct fluid-film stiffness coefficients ($\bar{S}_{xx}$) at different eccentricity ratios and speed parameters respectively in IHD and THD cases. As the fluid viscosity reduces due to rise in fluid temperature, the value of $\bar{S}_{xx}$ reduces when temperature effect is considered. The value of permeability parameter from which $\bar{S}_{xx}$ starts to reduce is observed to reduce as eccentricity ratio increases, especially this is more pronounced in THD case as compared to IHD case. As the viscous shear of fluid increases as the speed of journal increases, the fluid film temperature increases. This results into reduction of fluid viscosity and hence $\bar{S}_{xx}$ reduces as speed parameter increases when temperature effect is considered as shown in Fig. 4. However, in IHD case the viscosity of fluid remains constant since rise in fluid film temperature is not considered and as the fluid film pressure increases as speed of journal increases, $\bar{S}_{xx}$ increases as speed parameter increases. The influence of permeability of porous matrix is also observed to be dependents on speed parameter especially when temperature effect is considered.

Figures 5 and 6 show the variation of the direct fluid-film damping coefficient ($\bar{C}_{xx}$) with permeability of porous matrix at different eccentricity ratios and speed parameter respectively in IHD and THD analyses. As seen from Fig. 5, $\bar{C}_{xx}$ starts to reduce for the smaller value (less than 1E-02) of permeability parameter when thermal effect is considered while it shows this trend for slightly higher value of permeability parameter (more than 1E-03) when thermal effect is not considered. Similar trend can be observed in Fig. 6 at different speeds. This clearly indicates a coupled influence of permeability parameter and thermal effects on direct fluid film damping coefficient. The direct fluid-film damping coefficient $\bar{C}_{zz}$ is also found to show the same trend with permeability parameter at different eccentricity ratios and speed parameters and hence these results are not presented.

As seen from Fig. 7, the porous journal bearing provides improved stability threshold speed as compared to similar solid bearing. It further increases as permeability parameter increases in both IHD and THD cases. The stability threshold speed increases with eccentricity ratios when thermal effect is not considered (i.e. in IHD case) while it shows opposite trend when thermal effect is considered (i.e. in THD case). The range of permeability parameter from which $\bar{\omega}_{th}$ starts to increase is different in IHD and THD cases.

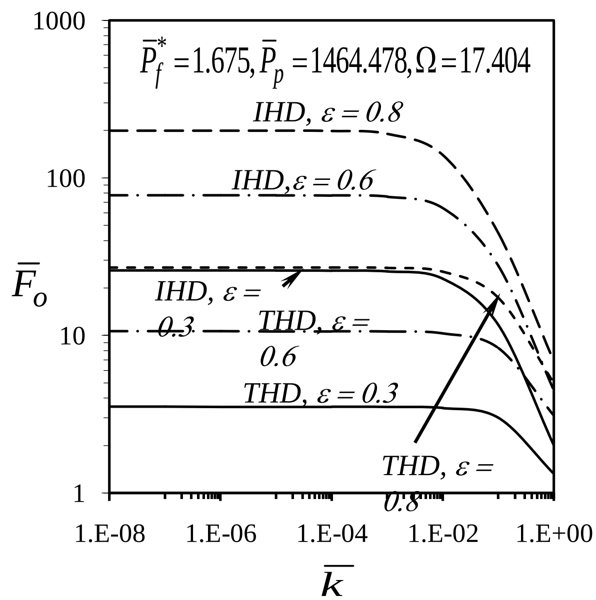

Fig. 1: Variation of load carrying capacity with permeability parameter and eccentricity ratio.

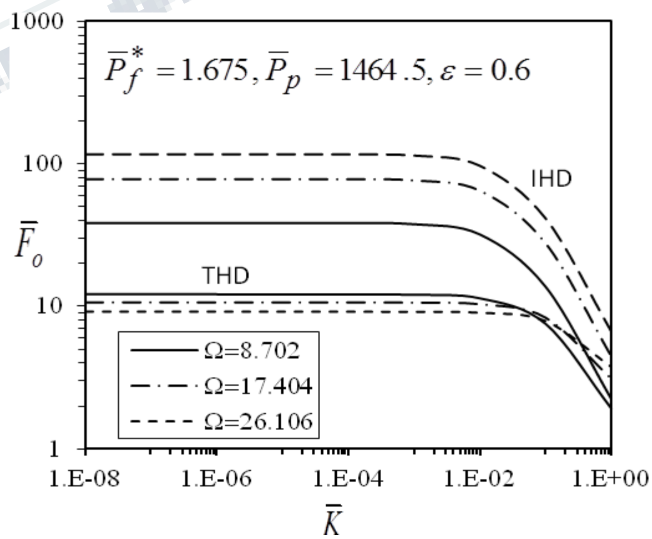

Fig. 2: Variation of load carrying capacity with permeability parameter and speed parameter.

ISSN (Online) 2456-1290
International Journal of Engineering Research in Mechanical and Civil Engineering
(IJERMCE)
Vol 2, Issue 4, April 2017

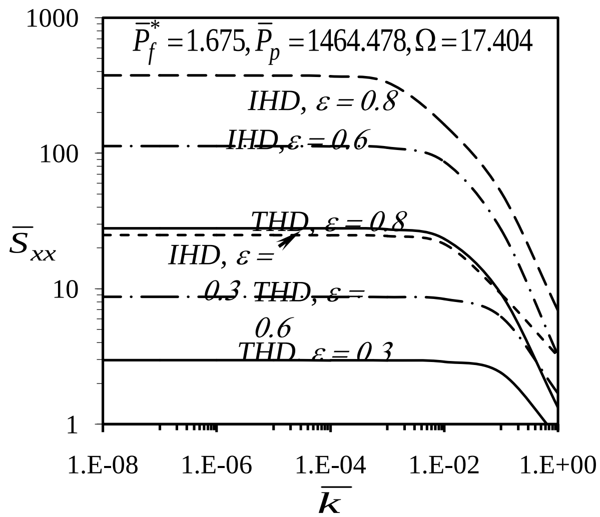

Fig. 3: Variation of direct stiffness coefficient $\bar{S}_{xx}$ with permeability parameter and eccentricity ratio

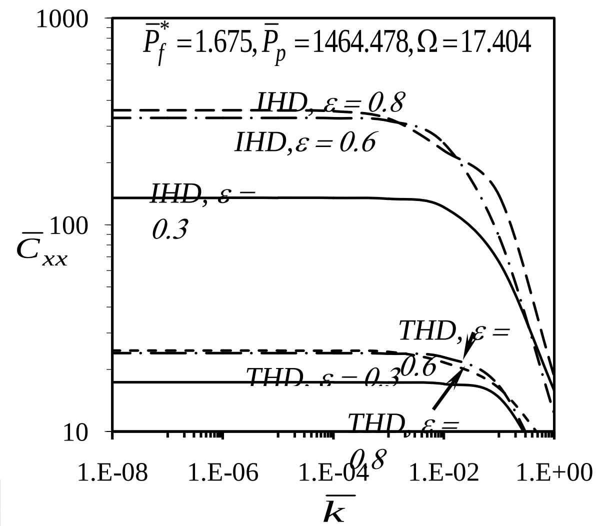

Fig. 5: Variation of direct damping coefficient $\bar{C}_{xx}$ with permeability parameter and eccentricity ratio

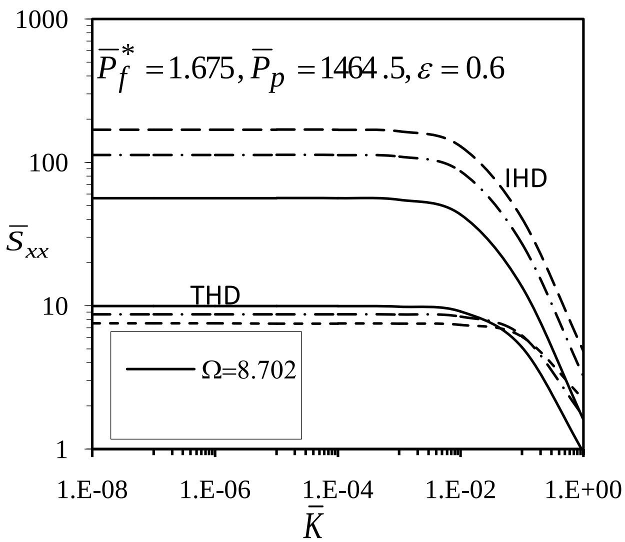

Fig. 4: Variation of direct stiffness coefficient $\bar{S}_{xx}$ with permeability parameter and speed parameter

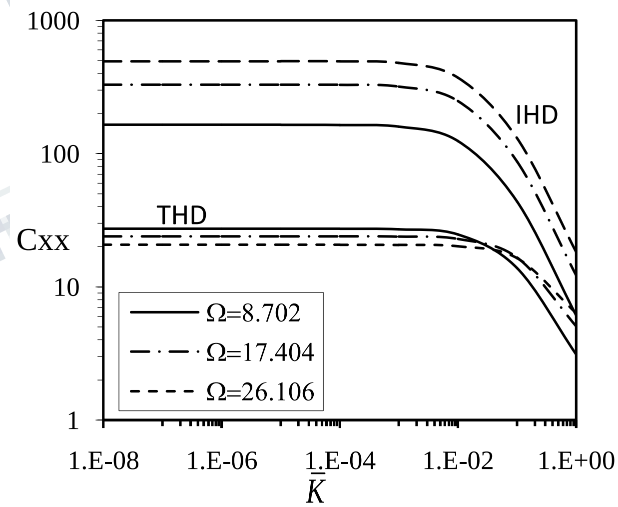

Fig. 6: Variation of direct damping coefficient $\bar{C}_{xx}$ with permeability parameter and speed parameter

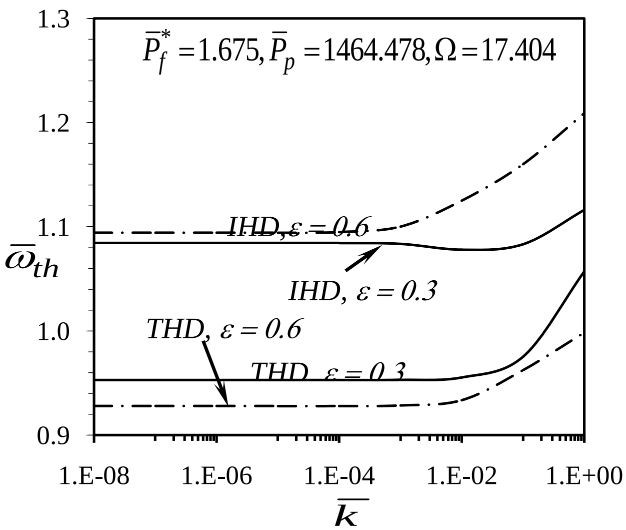

Fig. 7: Variation of stability threshold speed with permeability parameter and eccentricity ratio

IV. CONCLUSION

From the results presented in the previous section, the following conclusions are drawn:

1. The load carrying capacity ($\bar{F}_o$), direct fluid-film stiffness coefficient ($\bar{S}_{xx}$) and direct fluid-film damping coefficients ($\bar{C}_{xx}$ and $\bar{C}_{zz}$) reduces as permeability parameter increases. However, the value of permeability parameter that causes the significant reduction of the above performance characteristics is found to be more when temperature effect is considered.
2. The stability threshold speed parameter of journal bearing is found to increases as permeability parameter increases.
3. The influence of permeability parameter on load carrying capacity, fluid film stiffness and damping coefficients is found to couple with speed parameter, eccentricity ratios and temperature effect.

REFERENCES

[1] Lin J. R., and Hwang C. C., "Lubrication of Short Porous Journal Bearings-use of the Brinkman-Extended Darcy Model," Wear, vol. 161, pp 93-104, 1993.
[2] Reason B. R., and Siew A. H., "A Refined Numerical Solution for the Hydrodynamic Lubrication of Finite Porous Journal Bearings," Tribology Group, Proc. Instn. Mech. Engrs, vol. 199, pp 85-93, 1985.
[3] Guha S. K., "Linear Stability Performance Analysis of Finite Hydrostatic Porous Journal Bearings under the Coupled Stress Lubrication with the Additives Effects into Pores," Tribology International, vol. 43, pp 1294-1306, 2010.
[4] Naduvinamani N. B., and Siddangouda A., "Effect of Surface Roughness on the Hydrodynamic Lubrication of Porous Step-Slider Bearings with Couple Stress Fluids," Tribology International, vol. 40, pp 780-793, 2007.
[5] Naduvinamani N. B., and Patil S. B., "Numerical Solution of Finite Modified Reynolds Equation for couple Stress Squeeze Film Lubrication of Porous Journal Bearings," Computers and structures, vol. 87, pp 1287-1295, 2009.
[6] Lekaa H. Abd Al-shaheed., "Effect of Journal Misalignment on the Static Characteristics of Porous Journal Bearings Lubricated with Couple Stress Fluid," Al-Khwarizmi Engineering Journal, vol. 8, pp 42-53, 2012.
[7] Mak W. C., and Conway H. D., "Effects of Velocity Slip on the Elastohydrodynamic Lubrication of Short Porous Journal Bearings," International Journal Mechanical Science, vol. 20, pp 767-775, 1978.
[8] Abdallah A. Elsharkawy., and Lotfi H. Guedouar., "Hydrodynamic Lubrication of Porous Journal Bearing using a Modified Brinkman-Extended Darcy Model," Tribology International, vol. 34, pp 767–777, 2001.
[9] Abdallah A. Elsharkawy., and Lotfi H. Guedouar., "Direct and Inverse Solutions for Elastohydrodynamic Lubrication of Finite Porous Journal Bearing," Transactions of the ASME, vol. 123, pp 276-282.
[10] Boubendir S., Larbi., and Bennacer R., "Numerical Study of the Thermo-Hydrodynamic Lubrication Phenomena in Porous Journal Bearing," Tribology International, vol. 44, pp 1-8, 2011.

ISSN (Online) 2456-1290
International Journal of Engineering Research in Mechanical and Civil Engineering (IJERMCE)
Vol 2, Issue 4, April 2017

NOMENCLATURE

c : *Radial clearance, mm*
D : *Journal diameter, mm*
e : *Journal eccentricity, mm*
c_{pf}, c_{pp} : *Specific heat of fuel, porous material, J Kg*$^{-1}$ *K*$^{-1}$
k_p, k_j : *Thermal conductivity of porous bearing and journal, Wmm*$^{-1}$ *K*$^{-1}$
k_r : *Reference thermal conductivity of fluid*
T_f, T_p : *Temperature of fluid-film, porous bearing and journal, K*
T_r : *Reference temperature, K*
R_j, R_p : *Radius of journal, mm*
p_f, p_s : *Fluid-film pressure, supply pressure, N mm*$^{-2}$
μ_r : *Reference viscosity of lubricant, Pa s*
ρ_f, ρ_j, ρ_p : *Density of fluid, journal and porous materials, Kg m-3*

Non-dimensional Parameters

$\bar{C}_{ij} = C_{ij}\left(\dfrac{\omega_j c}{p_s R_j^2}\right)$, *Fluid-film damping coefficients*

$\bar{D}_f = \left(\dfrac{p_s}{\rho_f c_{pf} T_r}\right)$, *Dissipation number*

$\bar{F}_0, \bar{F}_1, \bar{F}_2 = F_0\left(\dfrac{\mu_r}{h}\right), F_1\left(\dfrac{\mu_r}{h^2}\right), F_2\left(\dfrac{\mu_r}{h^3}\right)$

$\bar{F}_{x,z} = F_{x,z} / p_s R_j^2$, *Fluid film reactions*

$\bar{h} = h/c$, *Fluid-film thickness*

$\bar{k} = k\dfrac{1}{c^2}$, *Permeability parameter*

$\bar{K}_{ep} = K_{ep}/K_r$

$\bar{M}_c = M_c\left(\dfrac{\omega_j^2 c}{p_s R_j^2}\right)$, *Critical journal mass*

$\bar{M}_j = M_j\left(\dfrac{\omega_j^2 c}{p_s R_j^2}\right)$, *Journal mass*

$\bar{p}_f, \bar{p}^* = (p_f, p^*)/p_s$, *Pressure in fluid, in porous*

$\bar{P}_p = \left(\dfrac{\rho_p c_{pp}}{k_r}\right)\left(\dfrac{c^2 p_s}{\mu_r}\right)$, *Peclet number for porous matrix*

$\bar{S}_{ij} = S_{ij}\left(c/p_s R_j^2\right)$, Fluid-film stiffness coefficients

$\bar{t} = t\omega_j$, Time

$\bar{T}_f, \bar{T}_p = (T_f, T_p)/T_r$, Temperature in fluid, porous media

$\bar{u}, \bar{v} = (u, v)(\mu_{rRJ} / c^2 p_s)$, Fluid-film velocity components

$\bar{u}^*, \bar{v}^*, \bar{w}^* = (u^*, v^*, w^*)\left(\mu_r R_j / c^2 p_s\right)$, Velocity components in porous media

$\alpha, \beta = (x, y)/R_j$, Circumferential and axial coordinates

$\Omega_j = \omega_j\left(\dfrac{\mu_r R_j^2}{c^2 p_s}\right)$, Speed parameter

$\lambda = L/D$, Aspect ratio

ε = e/c, Eccentricity ratio

$\bar{\mu} = \mu/\mu_r$, Absolute viscosity